

## Supporting Information

for *Adv. Energy Mater.*, DOI: 10.1002/aenm.202201132

### A Highly Sensitive Triboelectric Vibration Sensor for Machinery Condition Monitoring

*Hongfa Zhao, Mingrui Shu, Zihao Ai, Zirui Lou, Kit Wa Sou, Chengyue Lu, Yuchao Jin, Zihan Wang, Jiyu Wang,\* Changsheng Wu, Yidan Cao, Xiaomin Xu, and Wenbo Ding\**

## Supporting Information

### **A Highly Sensitive Triboelectric Vibration Sensor for Machinery Condition Monitoring**

*Hongfa Zhao, Mingrui Shu, Zihao Ai, Zirui Lou, Kit Wa Sou, Chengyue Lu, Yuchao Jin, Zihan Wang, Jiyu Wang\*, Changsheng Wu, Yidan Cao, Xiaomin Xu, Wenbo Ding\**

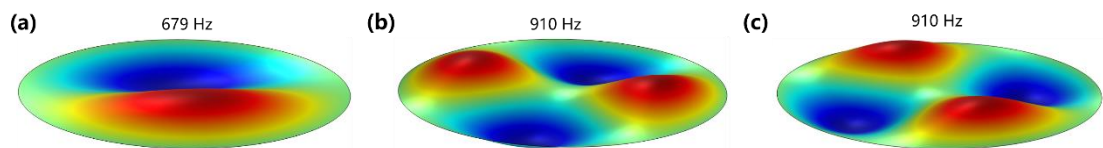


**Figure S1.** The third to fifth vibration mode of the FEP film. a) The third, b) the fourth and c) the fifth vibration mode of the FEP film.

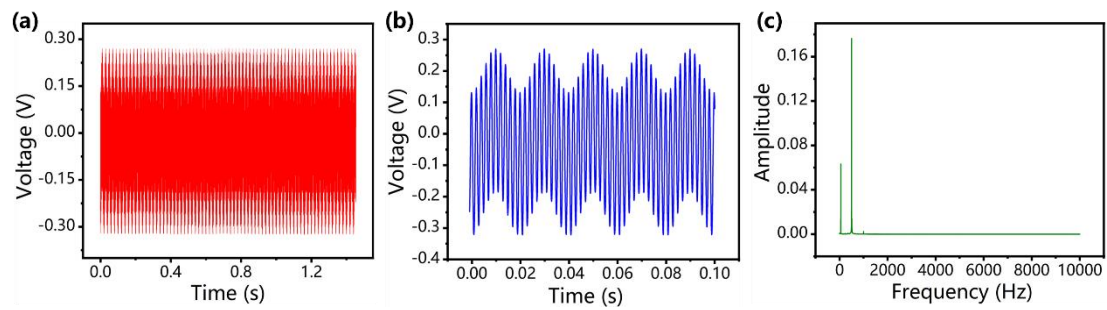


**Figure S2.** The voltage signals output by the VS-TENG at 500 Hz. a) The original voltage signals and b) The instantaneous voltage signals output by the TENG. c) The Fourier transform for voltage signals.

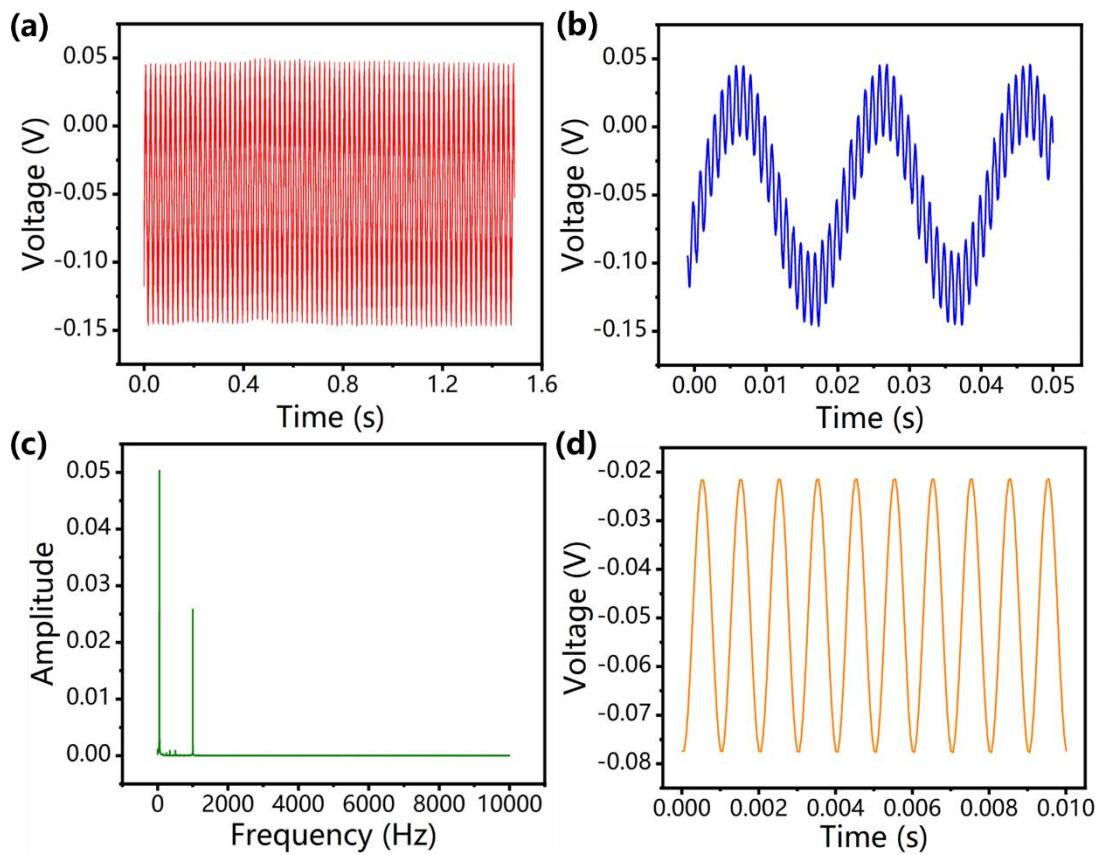


**Figure S3.** The voltage signals output by the VS-TENG at 1000 Hz. a) The original voltage signals and b) The instantaneous voltage signals output by the TENG. c) The Fourier transform for voltage signals. D) The filtered signals after bandpass filtering.

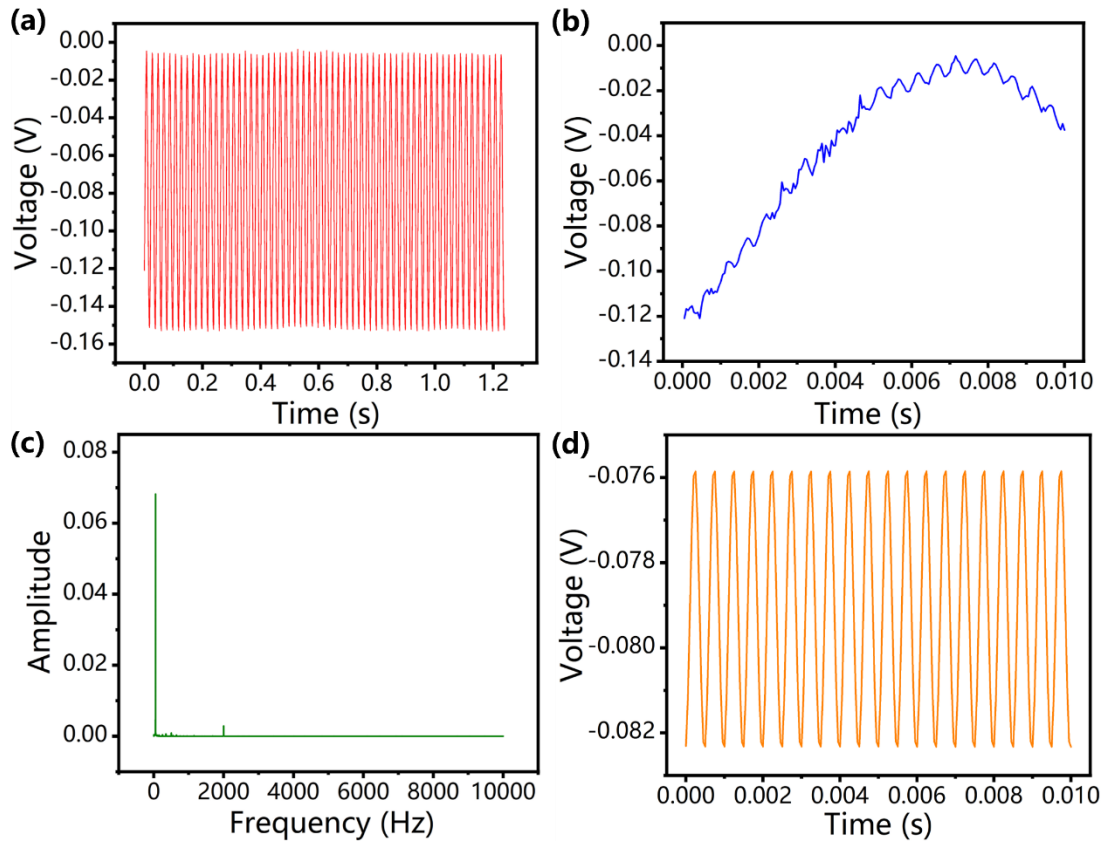


**Figure S4.** The voltage signals output by the VS-TENG at 2000 Hz. a) The original voltage signals and b) The instantaneous voltage signals output by the TENG. c) The Fourier transform for voltage signals. d) The filtered signals after bandpass filtering.

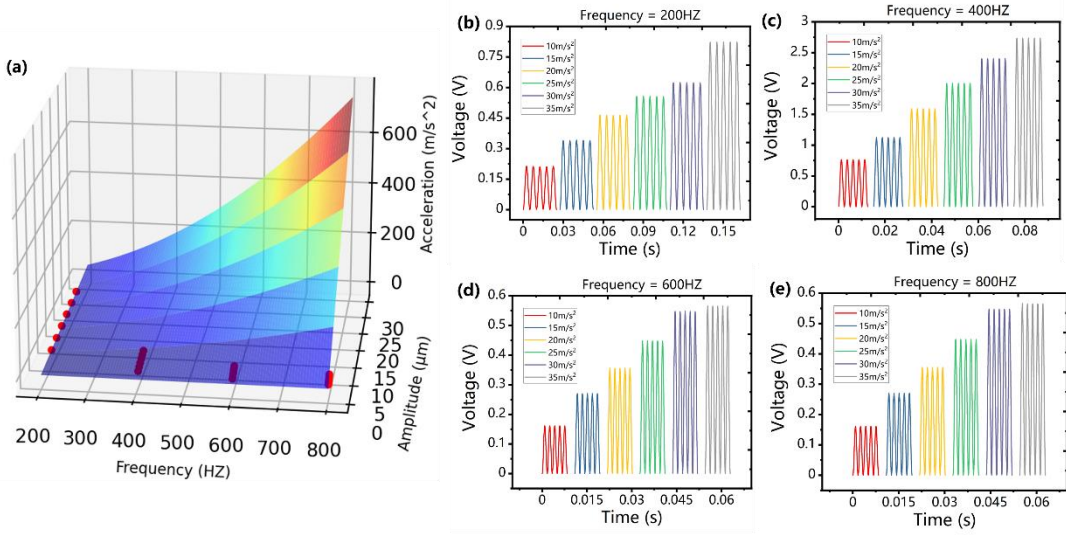


**Figure S5.** Open-circuit voltages output by the VS-TENG under different vibration conditions.  
 a) Relationship among vibration frequency, acceleration and amplitude. Variation of the open-circuit voltage with different accelerations from 10-35  $m/s^2$  at a fixed frequency of b) 200 Hz, c) 400 Hz, d) 600 Hz, and e) 800 Hz.

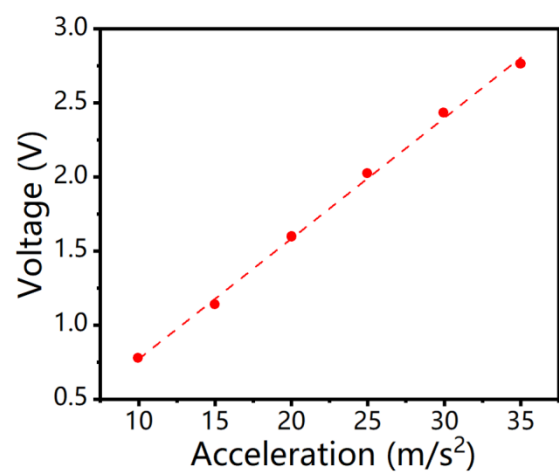


**Figure S6.** Linear fitting line of the relationship between voltage and acceleration.

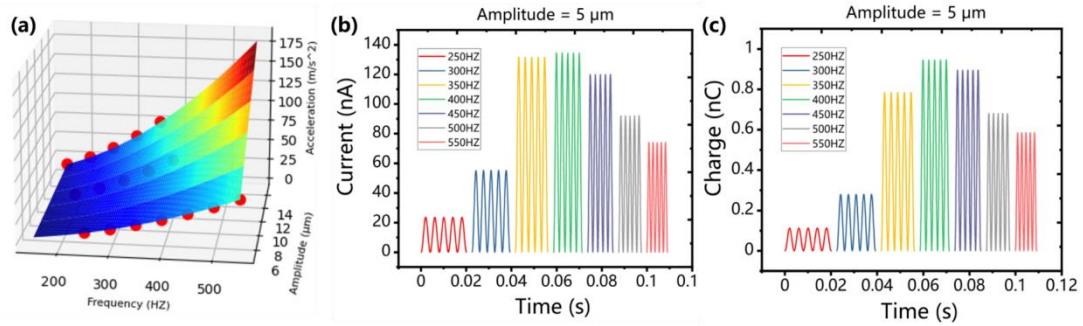


**Figure S7.** The output performance of the VS-TENG under different vibration frequencies. a) Relationships among vibration frequency, acceleration and amplitude. b) Short-circuit current and c) transferred charge signals output by the TENG with different frequencies from 250-550 Hz at a fixed amplitude of 5  $\mu\text{m}$ .

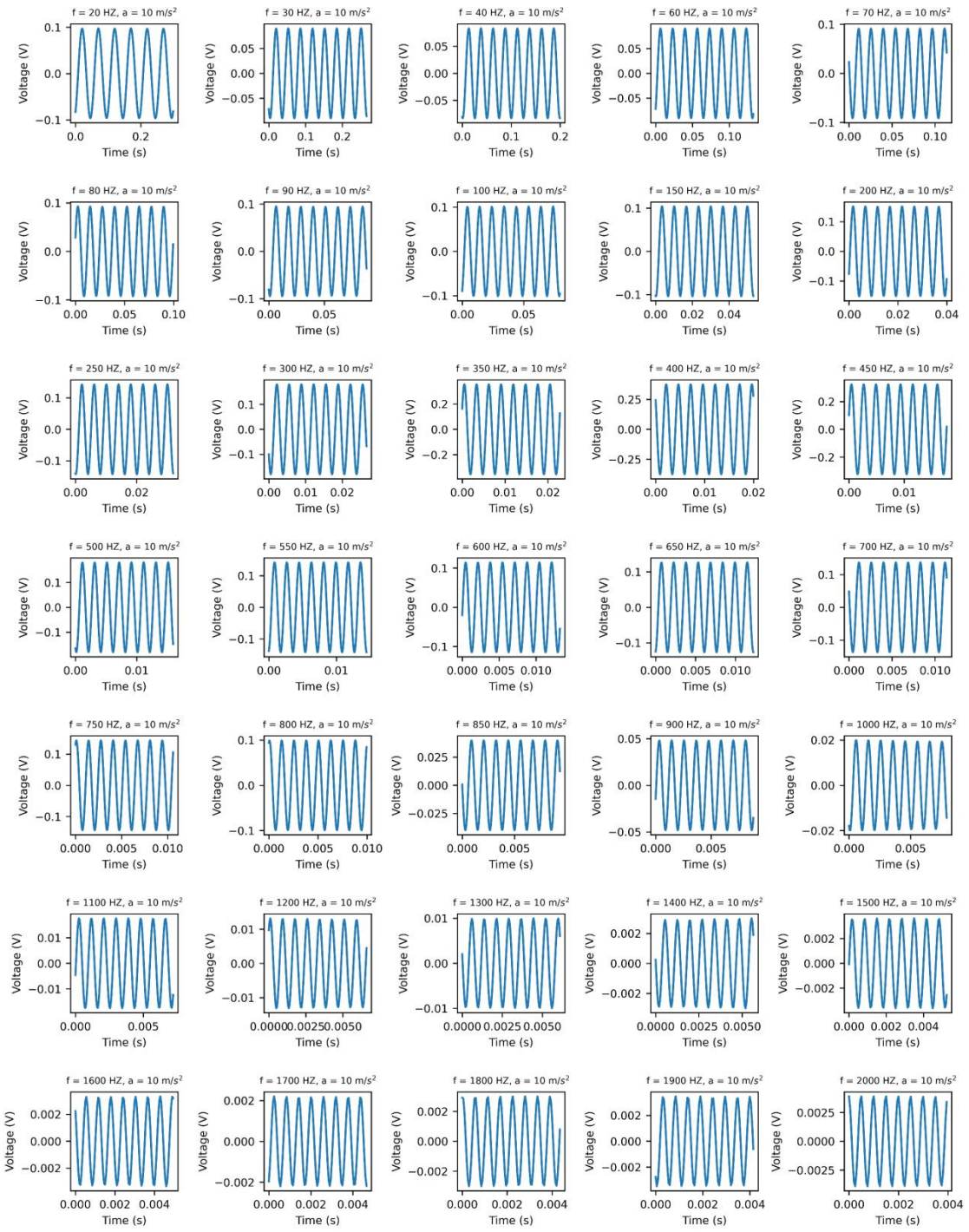


**Figure S8.** The open-circuit voltage of the VS-TENG under the vibration frequencies ranging from 20-2000 Hz and at an acceleration of  $10 \text{ m/s}^2$ .

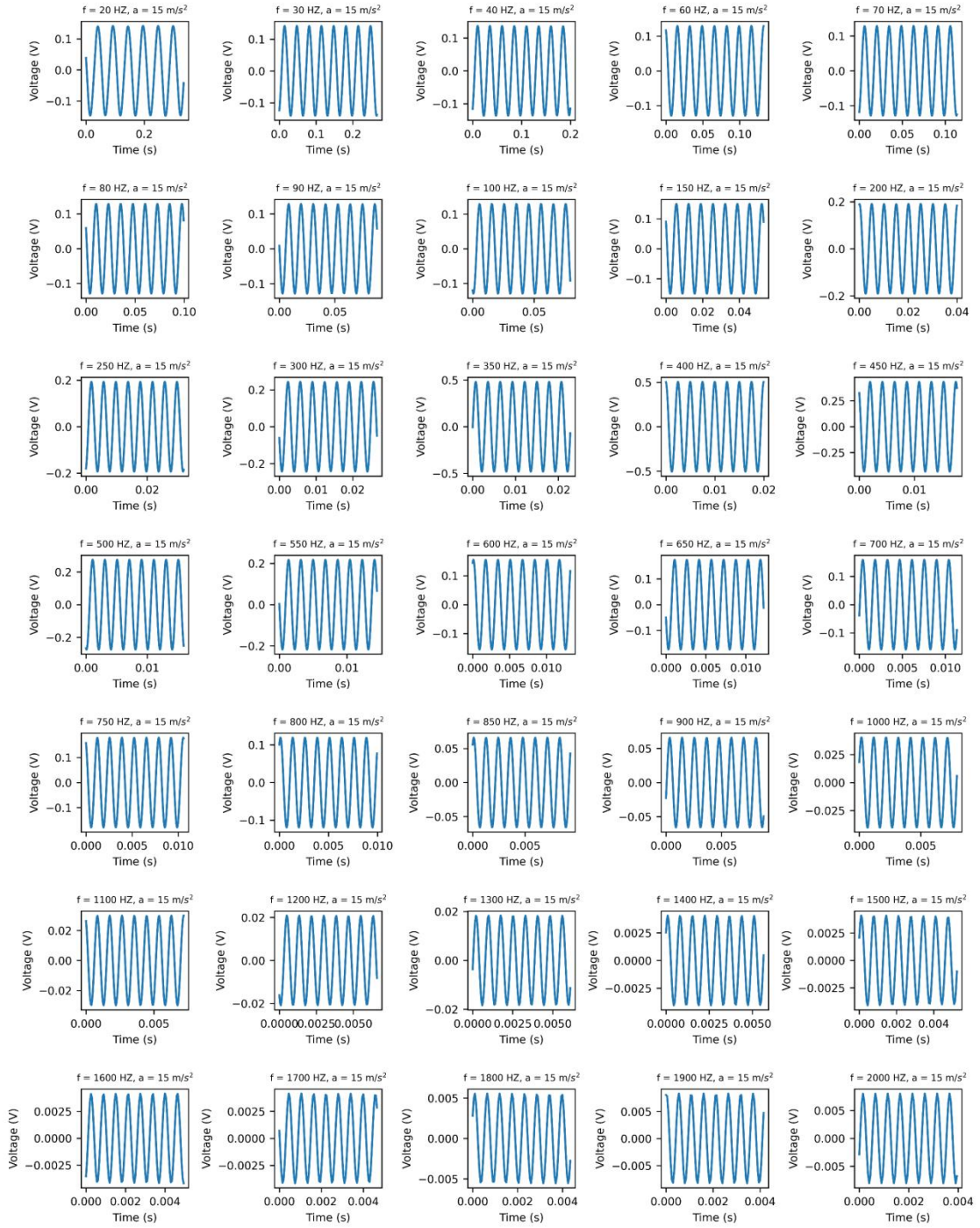


**Figure S9.**The open-circuit voltage of the VS-TENG under the vibration frequencies ranging from 20-2000 Hz and at an acceleration of  $15 \text{ m/s}^2$ .

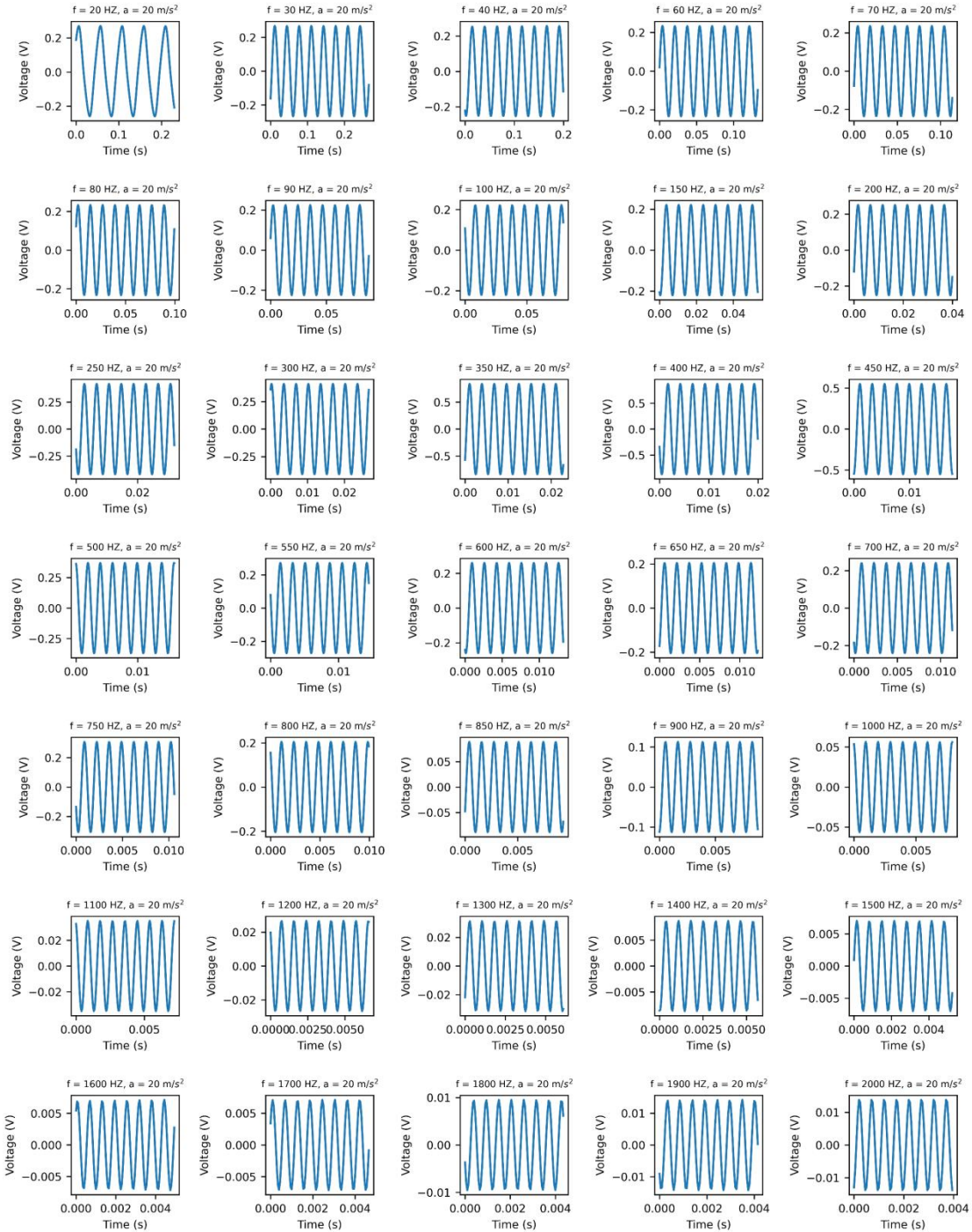


**Figure S10.** The open-circuit voltage of the VS-TENG under the vibration frequencies ranging from 20-2000 Hz and at an acceleration of  $20 \text{ m/s}^2$ .

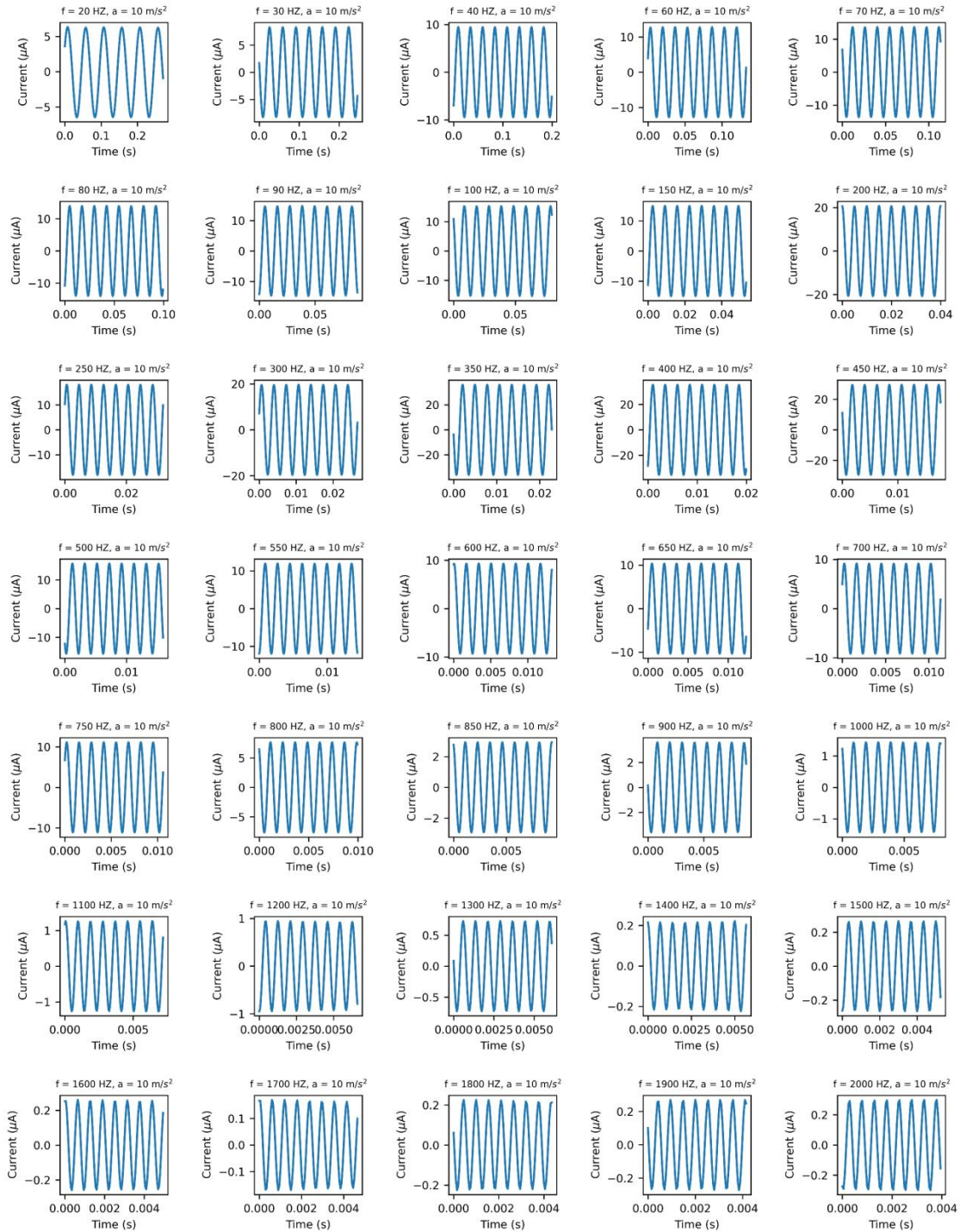


**Figure S11.** The short-circuit current of the VS-TENG under the vibration frequencies ranging from 20-2000 Hz and at an acceleration of  $10 \text{ m/s}^2$ .

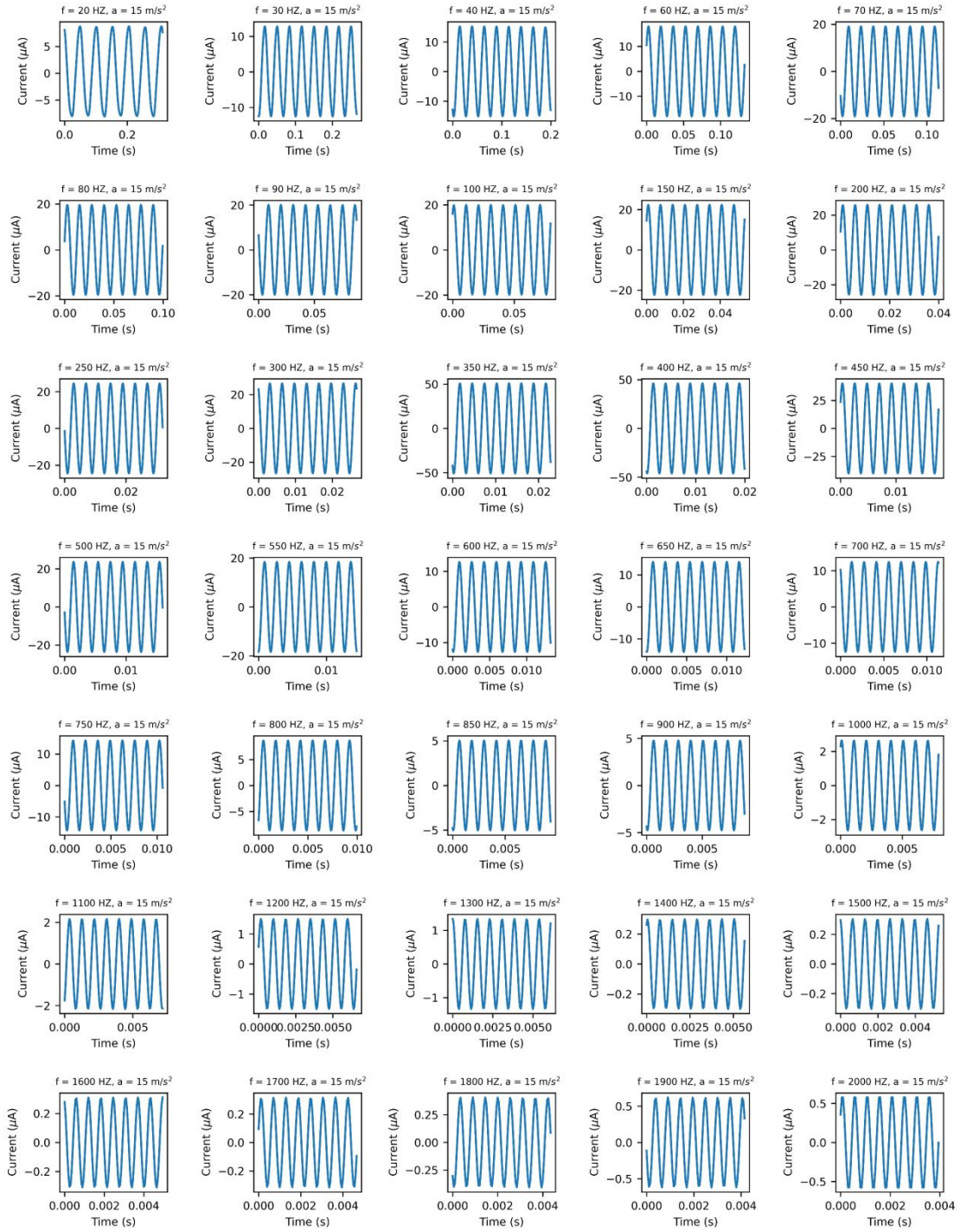


**Figure S12.** The short-circuit current of the VS-TENG under the vibration frequencies ranging from 20-2000 Hz and at an acceleration of  $15 \text{ m/s}^2$ .

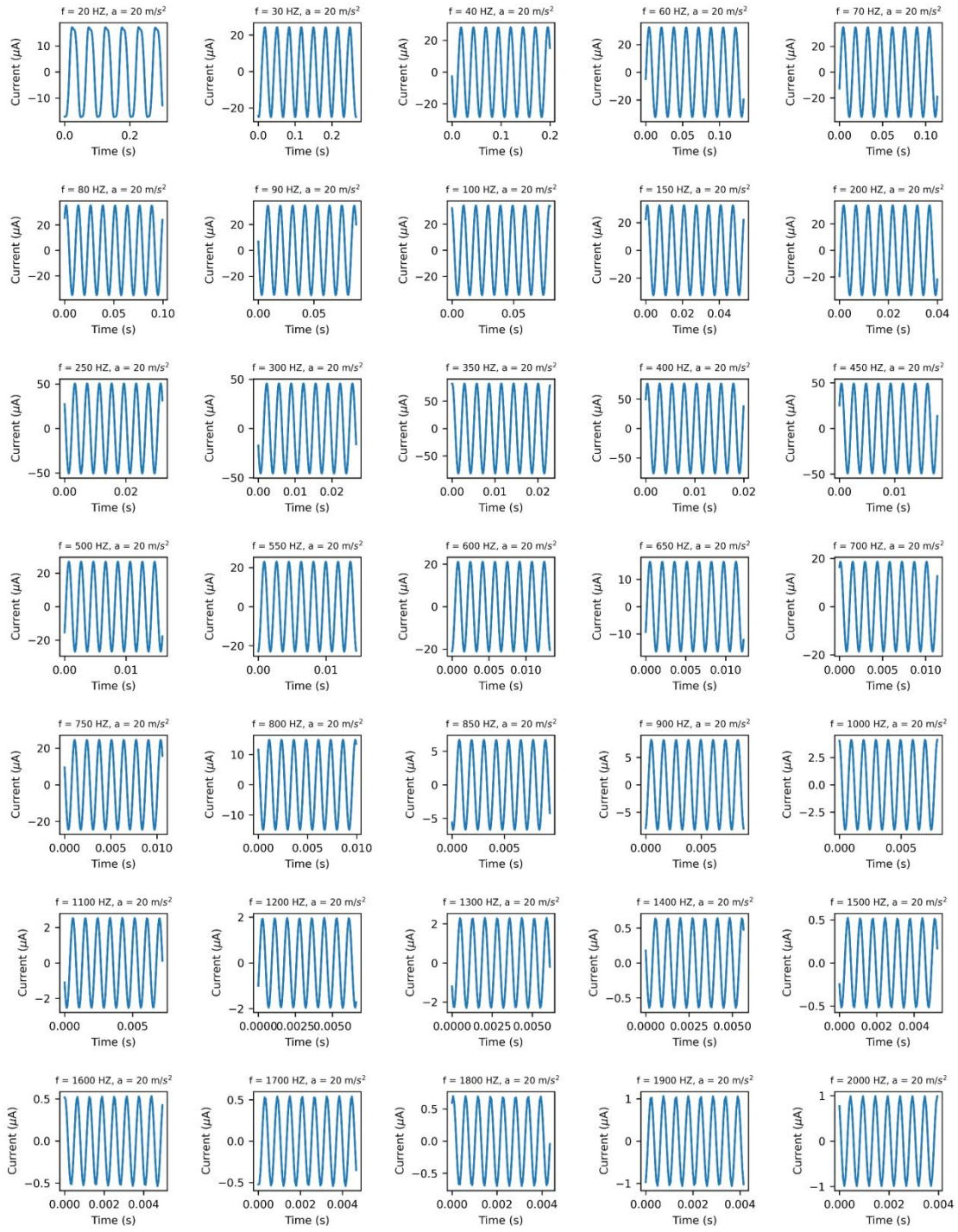


**Figure S13.** The short-circuit current of the VS-TENG under the vibration frequencies ranging from 20-2000 Hz and at an acceleration of  $20 \text{ m/s}^2$ .

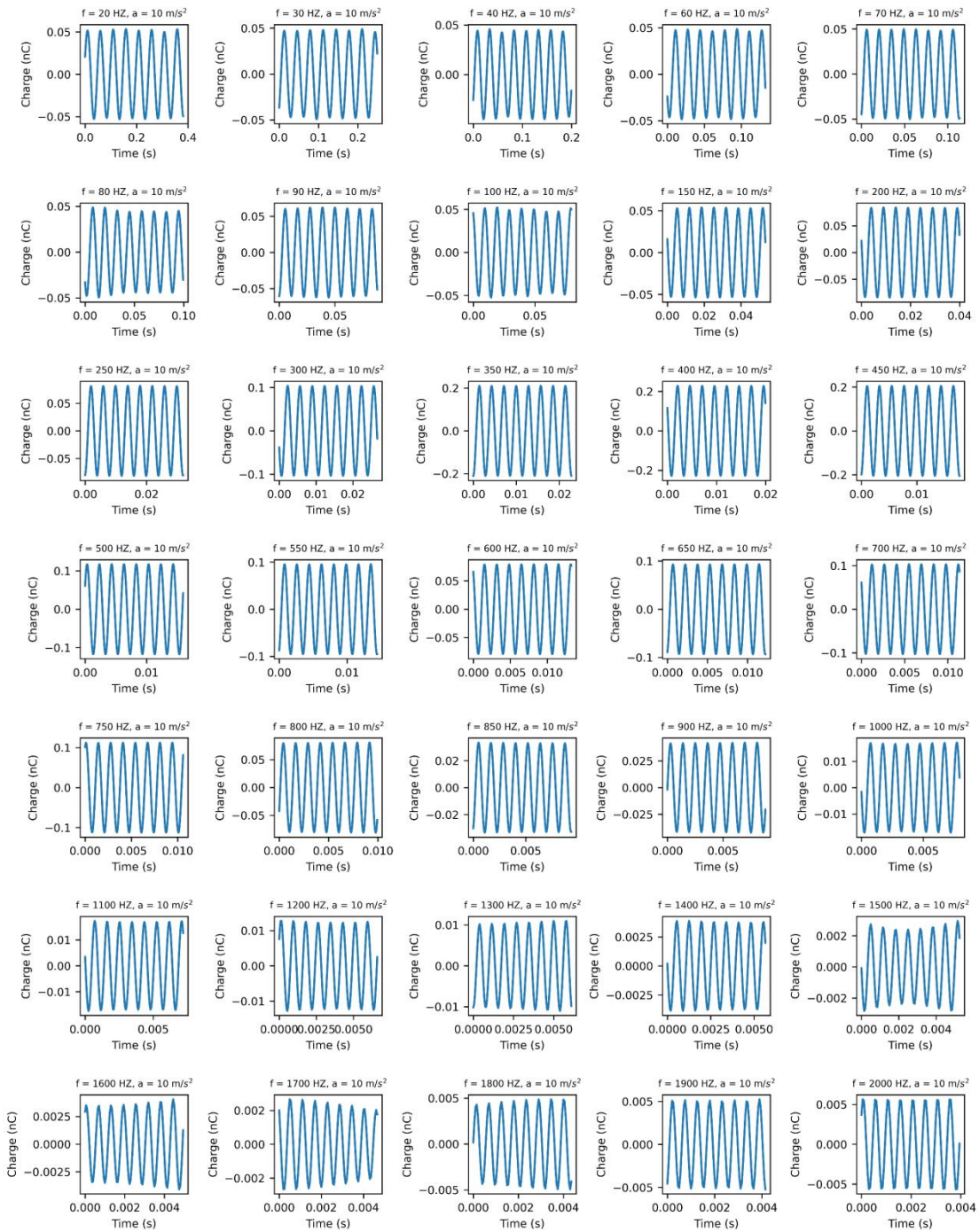


**Figure S14.** The short-circuit transferred charge of the VS-TENG under the vibration frequencies ranging from 20-2000 Hz and at an acceleration of  $10 \text{ m/s}^2$ .

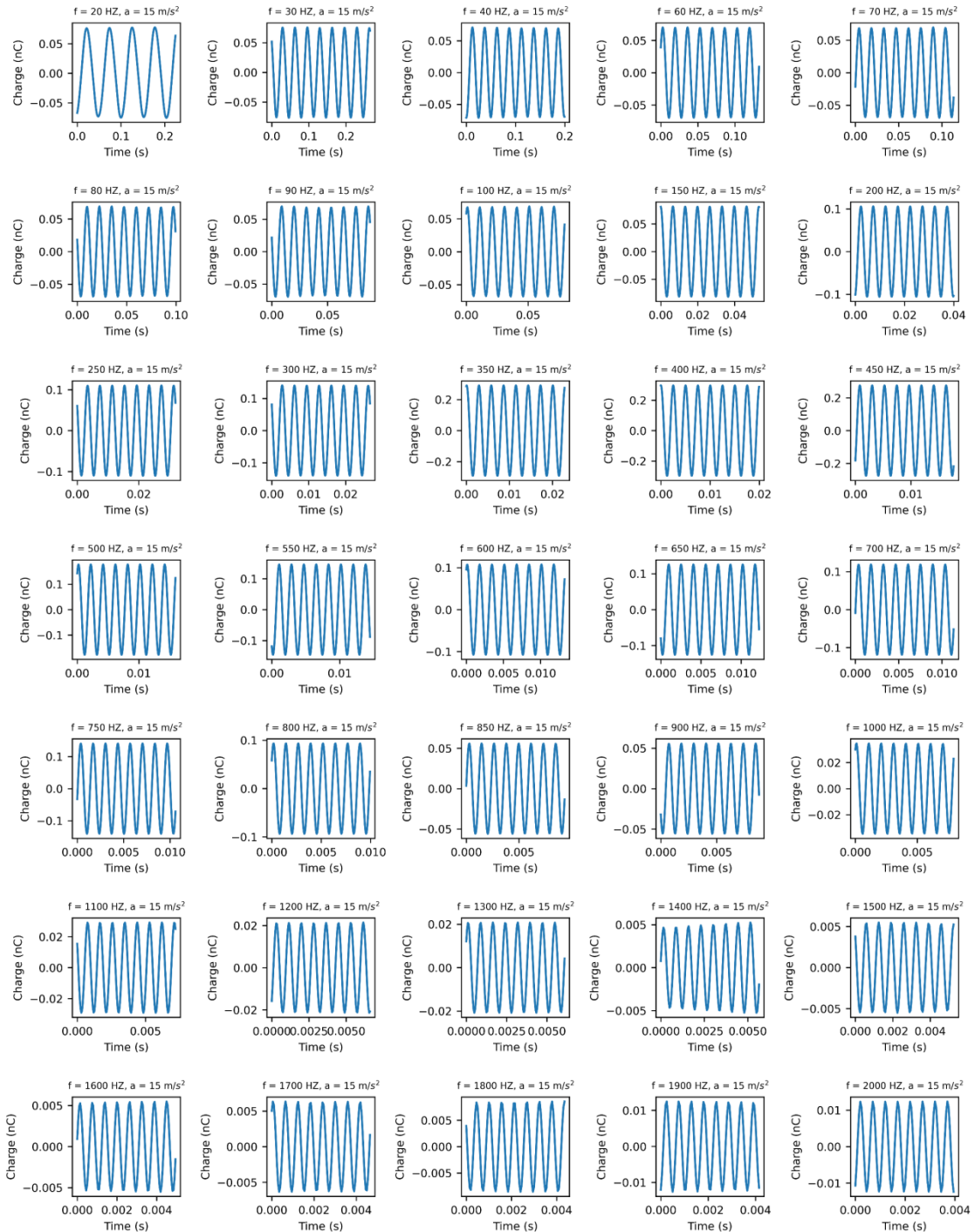


**Figure S15.** The short-circuit transferred charge of the VS-TENG under the vibration frequencies ranging from 20-2000 Hz and at an acceleration of 15 m/s<sup>2</sup>.

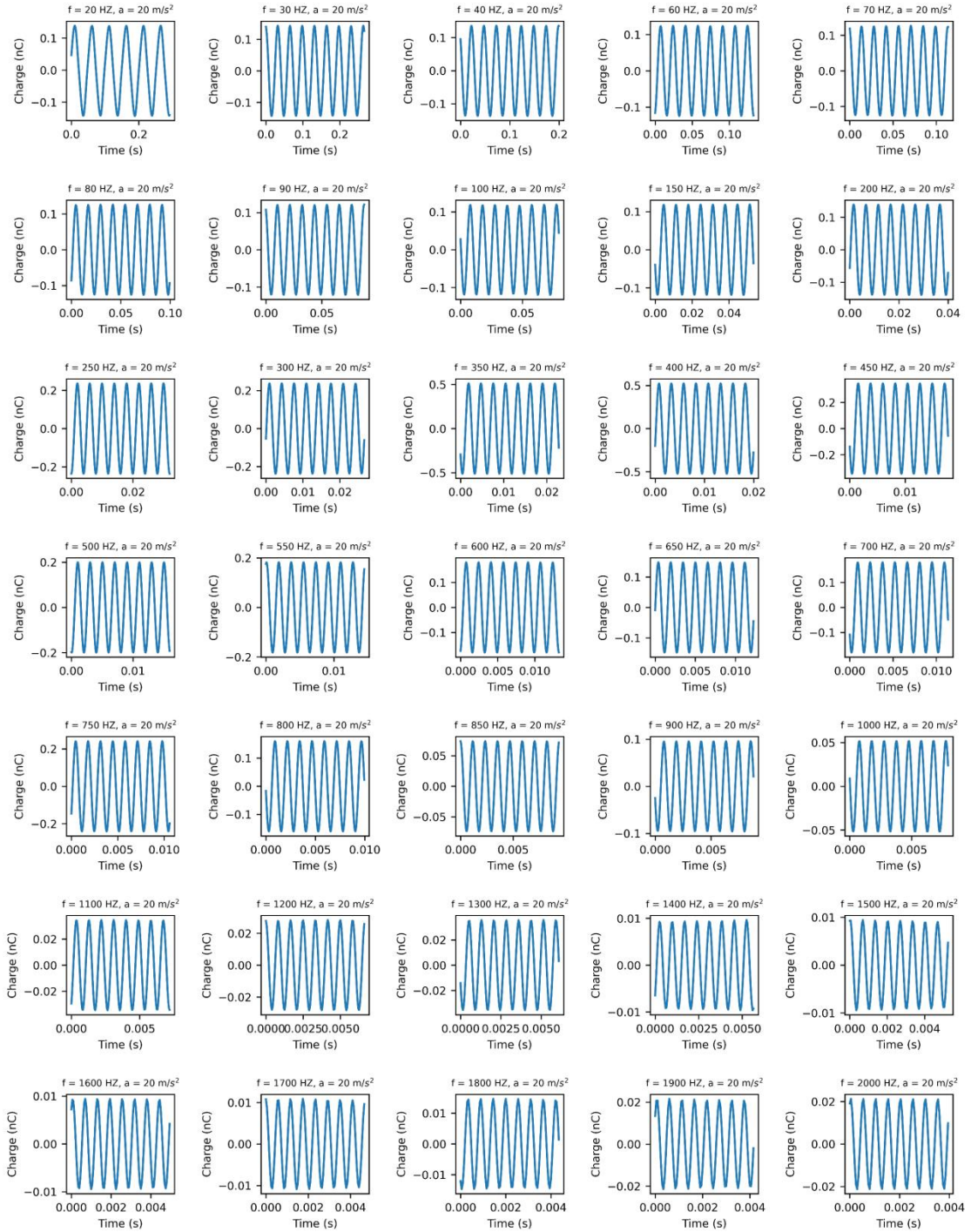


**Figure S16.** The short-circuit transferred charge of the VS-TENG under the vibration frequencies ranging from 20-2000 Hz and at an acceleration of  $20 \text{ m/s}^2$ .

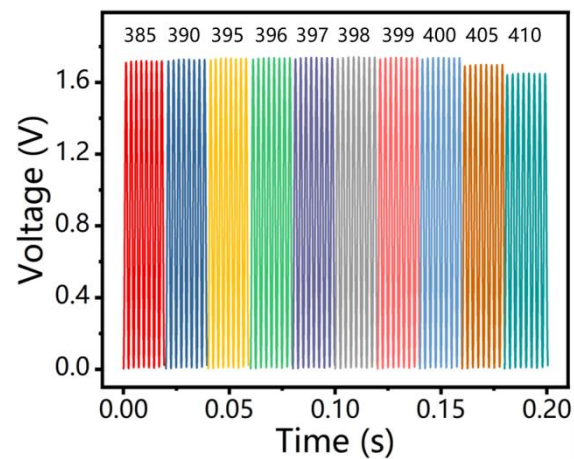


**Figure S17.** The instantaneous voltage signals from 385 Hz to 410 Hz with an acceleration of  $15 \text{ m/s}^2$ .

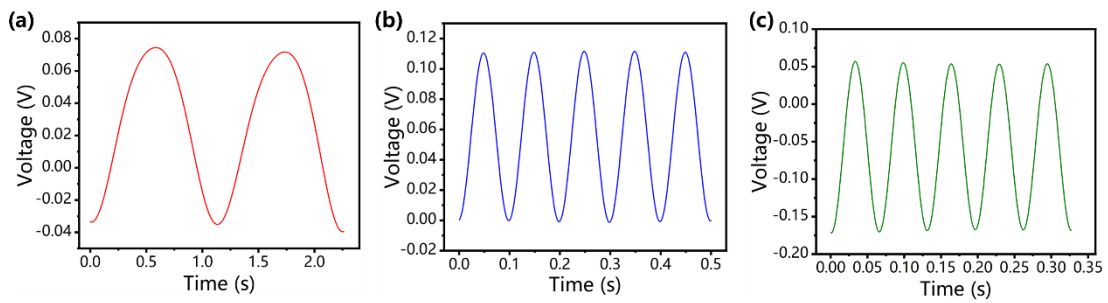


**Figure S18.** Output performance of the VS-TENG at lower frequencies. The voltage signals output by the TENG at the frequencies of a) 1 Hz, b) 10 Hz, and c) 15 Hz.

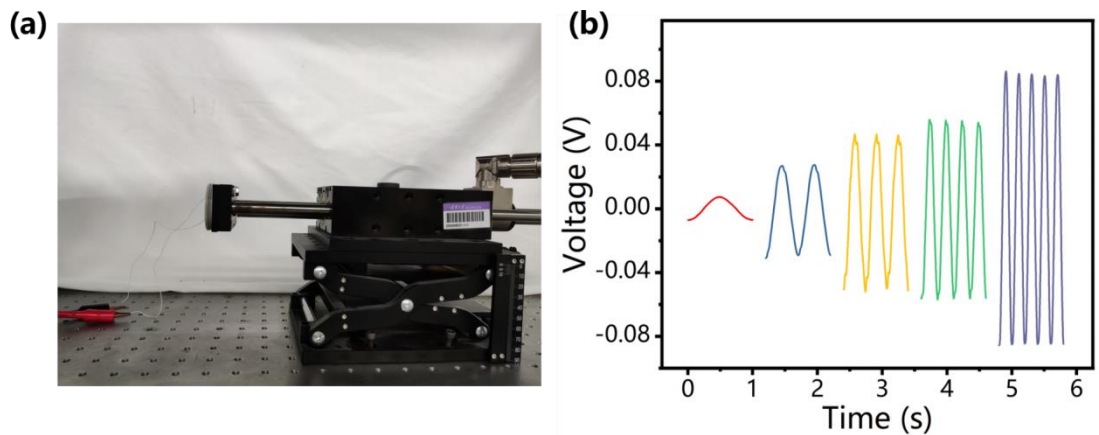


**Figure S19.** a) Photograph of the experiment. b) The voltage signals of the TENG at the frequency of 1-5 Hz.

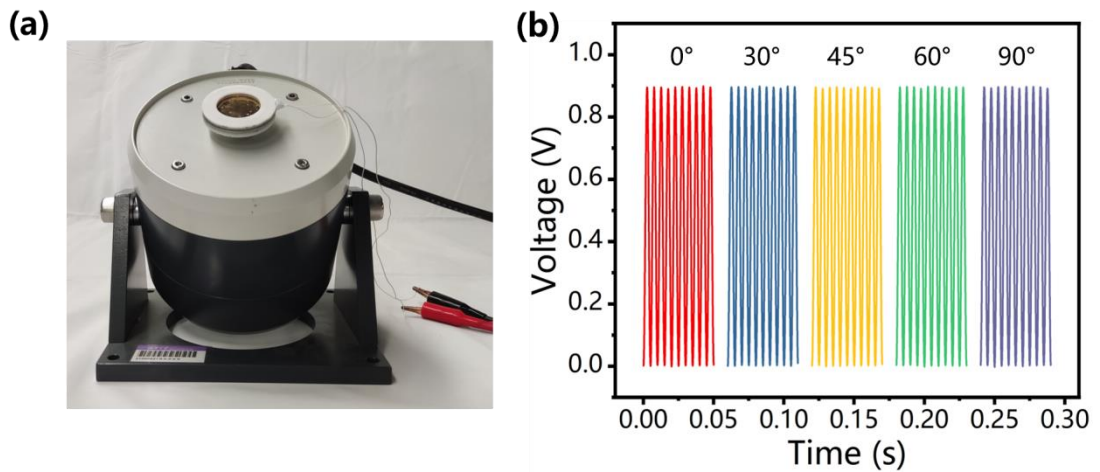


**Figure S20.** a) Photograph of the experiment. b) The voltage signals of the TENG when the vibration direction varies from  $0^\circ$  to  $90^\circ$ .

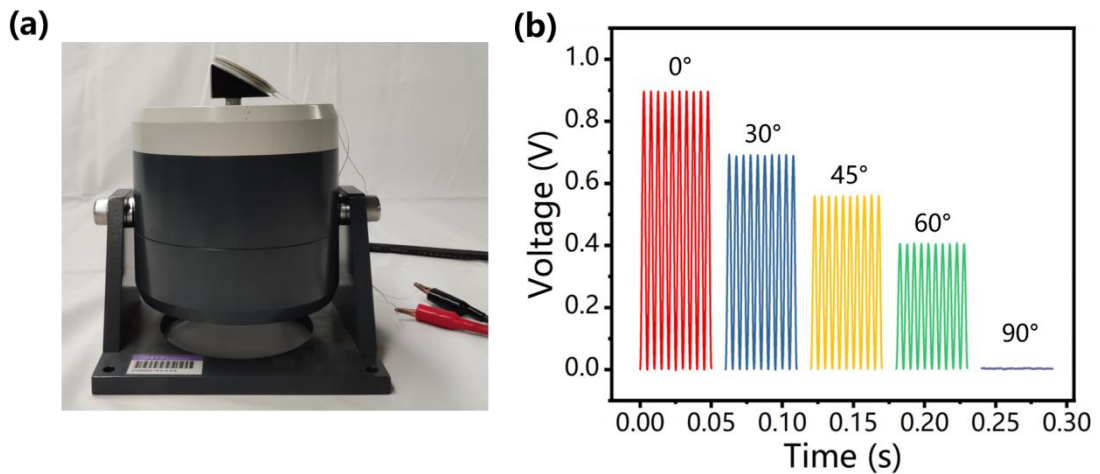


**Figure S21.** a) Photograph of the experiment. b) The voltage of the TENG when the angle between the TENG and vibration source changes.

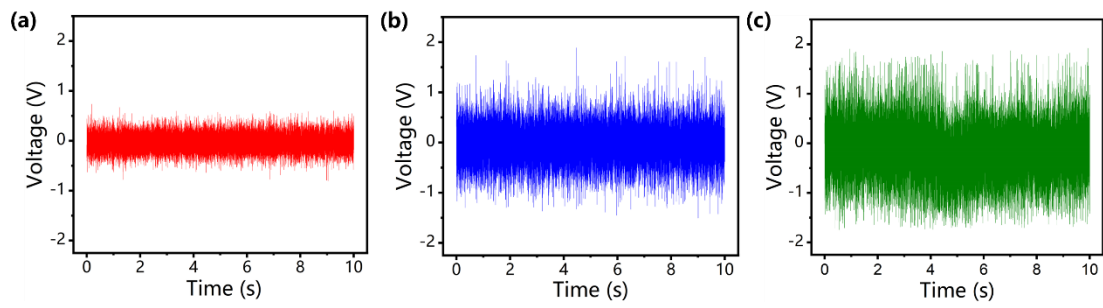


**Figure S22.** The voltage signals of the VS-TENG for the entire duration. The voltage signals output by the VS-TENG with the gear box operating at a) low speed, b) medium speed, and c) rated speed.

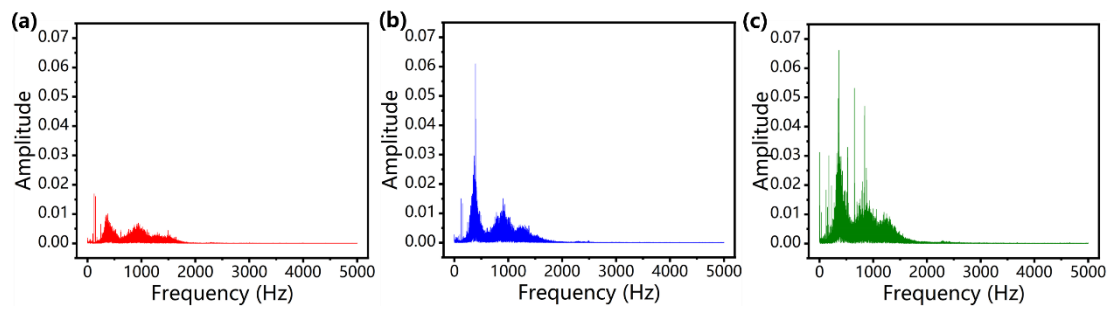


**Figure S23.** Frequency-domain signals when the gear box operates in forward rotation. Spectrum obtained after Fourier transform for the voltage signals output by the VS-TENG with the gear box in a) low speed, b) medium speed and c) rated speed.

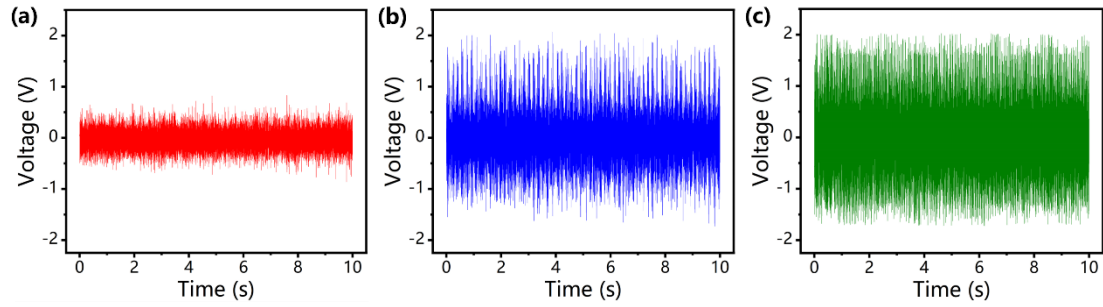


**Figure S24.** The voltage signals output by the VS-TENG when the gear box operates in reverse rotation. The voltage signals output by the TENG with the gear box operating at a) low speed, b) medium speed, and c) rated speed.

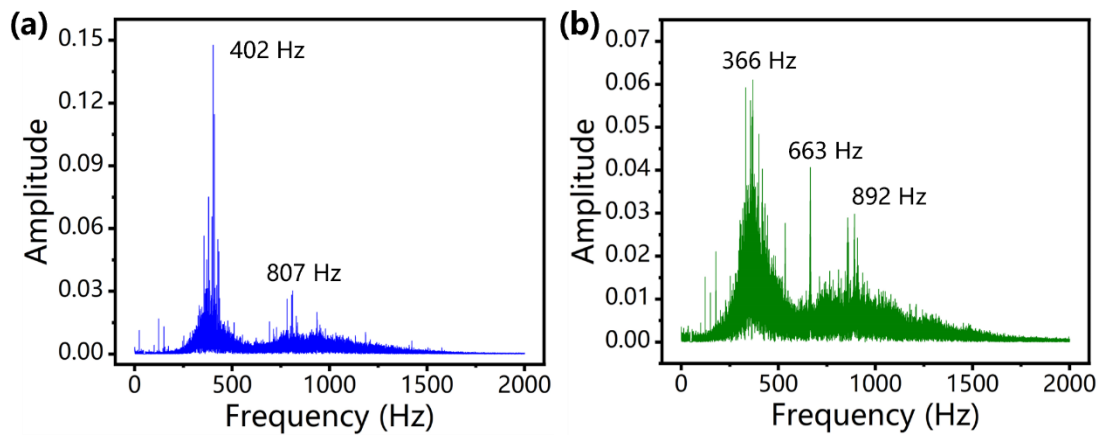


**Figure S25.** Frequency-domain signals when the gear box operates in reverse rotation. Spectrum obtained after Fourier transform for the voltage signals output by the VS-TENG with the gear box in a) medium speed and b) rated speed.

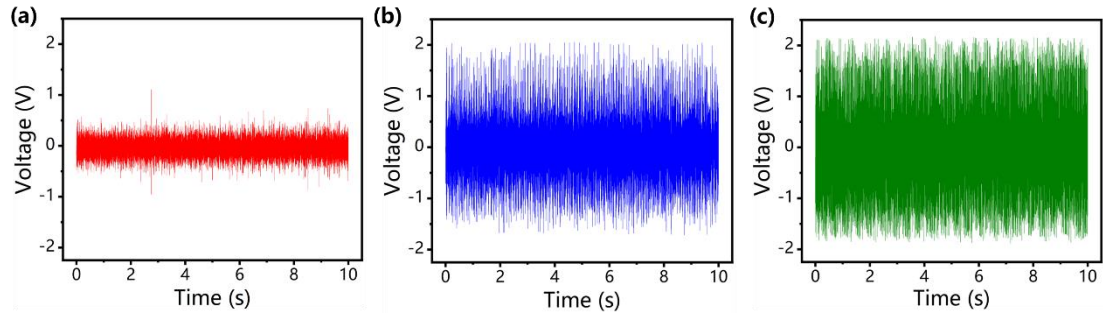


**Figure S26.** The voltage signals output by the VS-TENG when the gear box operates in shaft-misalignment condition. The voltage signals output by the TENG with the gear box operating at a) low speed, b) medium speed, and c) rated speed.

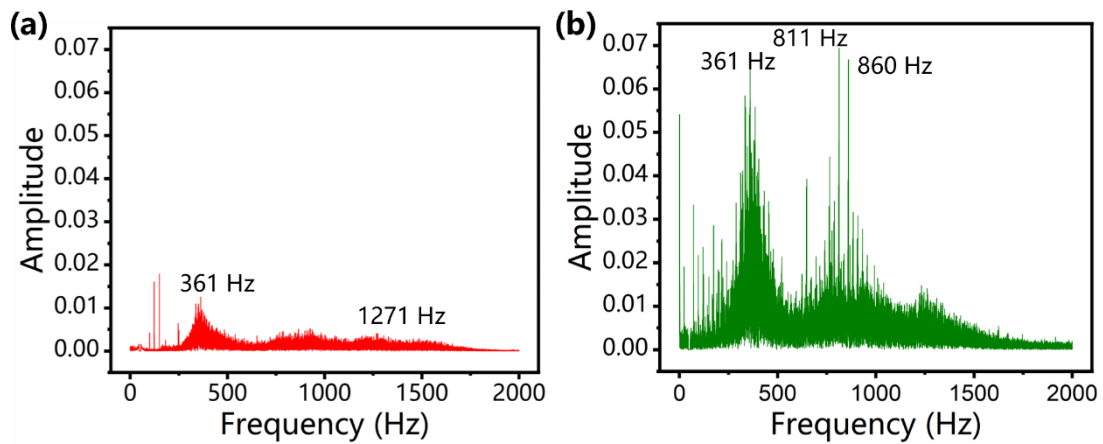


**Figure S27.** Frequency-domain signals when the gear box operates in shaft-misalignment condition. Spectrum obtained after Fourier transform for the voltage signals output by the VS-TENG with the gear box in a) low speed and b) rated speed.

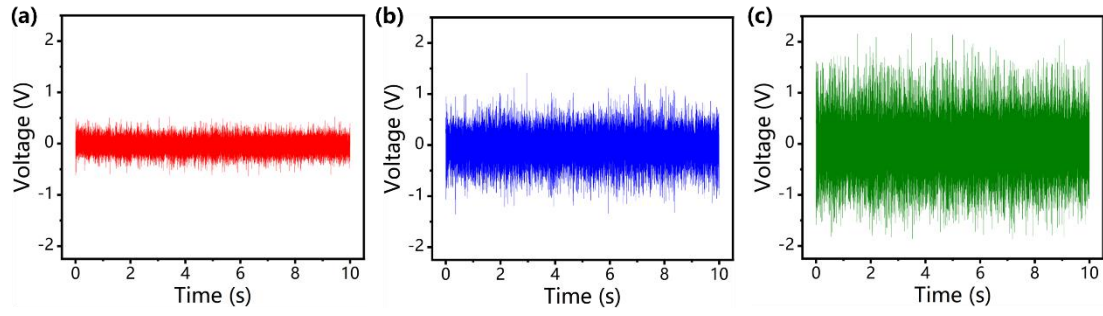


**Figure S28.** The voltage signals output by the VS-TENG when the gear box operates with a faulty coupling. The voltage signals output by the TENG with the gear box operating at a) low speed, b) medium speed, and c) rated speed.

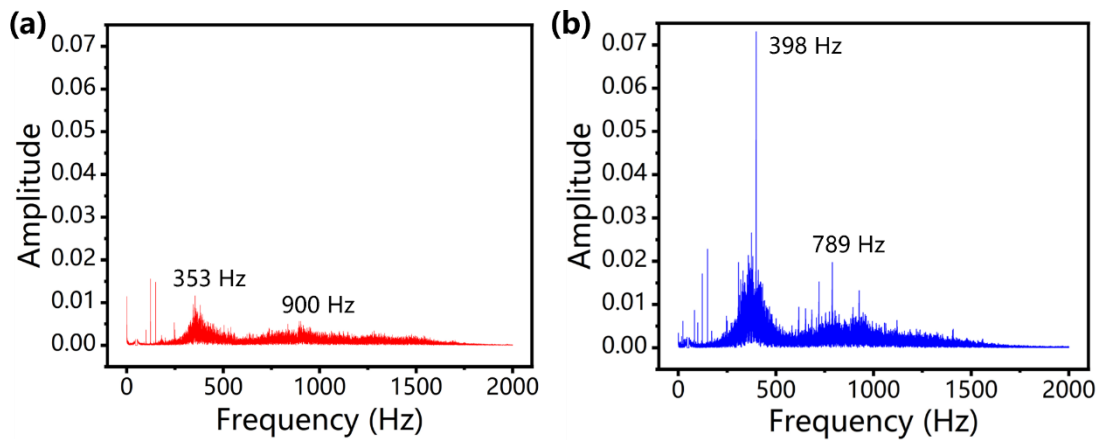


**Figure S29.** Frequency-domain signals when the gear box operates with a faulty coupling. Spectrum obtained after Fourier transform for the voltage signals output by the VS-TENG with the gear box in a) low speed and b) rated speed.

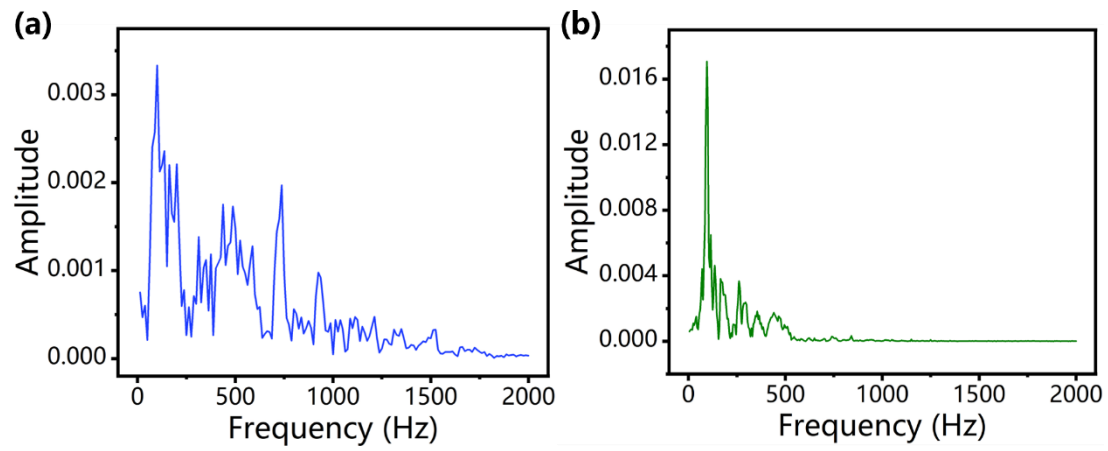


**Figure S30.** Fourier Transform of the voltage signals measured during the compressor in a) starting and b) closing period.

Table R1. Comparison between the related works.

	Time	Author	TENG name	Tribo-charge layers	Detection range	Application scenarios
1	2013	Chen <sup>1</sup>	V-TENG	Al, PTFE	2-200 Hz	Hand slapping
2	2014	Wang <sup>31</sup>	CF-TENG	Al, FEP	1-80 Hz, 3.5 $\mu\text{m}$ at 15 Hz	Wind blower
3	2017	Xu <sup>16</sup>	S-TENG	Silicon rubber, carbon	5-30 Hz, 2 m/s <sup>2</sup>	Vehicle vibration
4	2017	Wang <sup>2</sup>	SCPU	Al, FEP	2-40 Hz	Bicycle vibration
5	2017	Yu <sup>17</sup>	FTENG	Silicon rubber, FEP	Below 5 Hz, 1 cm	Bridge vibration monitoring
6	2017	He <sup>39</sup>	SG-TENG	Al, PTFE	10-180 Hz	Boxing training
7	2017	Zhao <sup>30</sup>	TEVA	Al, Kapton	2-12 Hz, 1.07 m/s <sup>2</sup>	Railway health
8	2019	Xiao <sup>32</sup>	HSI-TENG	Cu, PTFE	10-60 Hz, 1 mm	Engine condition monitoring
9	2020	Li <sup>33</sup>	V-TENG	Cu, PET	1-40 Hz 0.1 mm	Machine fault detection
10	2020	Bhatta <sup>40</sup>	MRSMS-HNG	Al, PEFE	1-10 Hz 2 m/s <sup>2</sup>	Arbitrary motion sensor
11	2020	Li <sup>26</sup>	AC/DC-TENG	FE, TEL	1.25-5.6 Hz 1 mm	Bridge monitoring
12	2021	Zhang <sup>4</sup>	TENG-SES	Carbon, TPU	<10 Hz	Infrastructure monitoring
13	2022	Zhang <sup>41</sup>	P-TENG	Cu, FEP	6-20 Hz	Internet of things
14	2022	Wu <sup>42</sup>	S-TENG	Cu, PTFE	1-50 Hz, 0.2 mm	Transmission lines
15	2022	Wang <sup>43</sup>	SUVS	CSP, HMM	1-315 Hz	Guitar vibration
16	Present	Zhao	VS-TENG	Foamed aluminum, FEP	1-2000 Hz, ~sub- $\mu\text{m}$	Mechanical equipment

### Supplementary Note S1. Detailed description of ITO and paper materials.

The ITO membranes with PET substrates (ITO 10  $\mu\text{m}$ , PET 115  $\mu\text{m}$ ) are used as the protection layers to protect the internal structure of the TENG, especially the FEP film and the gold printed electrode, which are easily damaged by external hard objects or improper manipulations. To avoid external physical damage may be a reason for the high durability and stability of the TENG. Also, since ITO is conductive, it acts as an electrostatic shield on the outer layer of TENG. But it is not enough when the noises in environment are large, so the digital filter is used together to filter out the noises.

The ITO with the PET substrate is not very fragile in the vibration frequency of 1-2000 Hz. After vibration testing, there is no crack damage on the surface of the ITO material, which is the same as the surface before the test (Figure N1). In fact, ITO can be replaced by other conductive materials like metals, and we can determine this material according to the application scenario. Here, the reason to use ITO is mainly because it's transparent and lightweight, and the internal structure of the TENG can be intuitively displayed so that if there is damage inside the TENG, we can find and repair it in time.

Paper is used as a spacer layer since it is lightweight, environmentally friendly, low cost, easy to shape and compatible with other materials. In fact, it can also be replaced by other materials according to actual application scenarios.

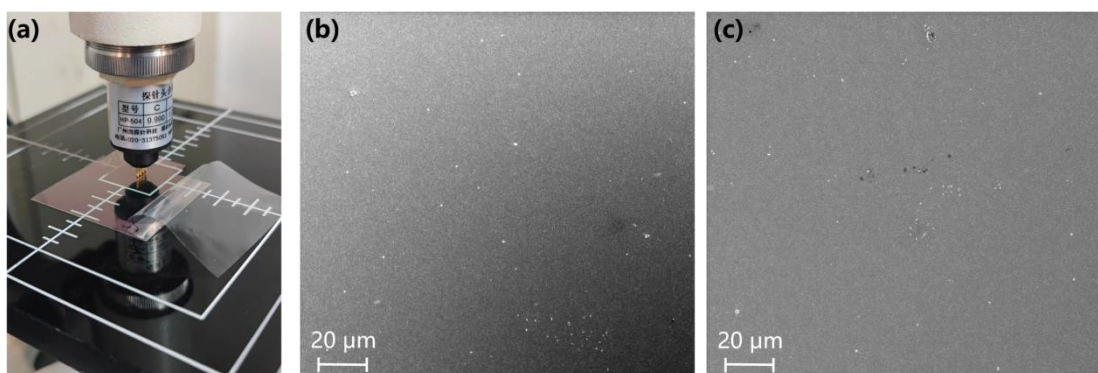


**Figure N1.** a) Photograph of the experiment process. SEM photos of b) the original ITO surface and c) the ITO surface after vibration testing.

## **Supplementary Note S2. The comparison of the electrical signals output by the TENGs using different electrodes.**

The aluminum and FEP materials are often used for fabricating TENGs due to their strong electropositivity and electronegativity. In the related references (Wang *et al.* *ACS Nano*. 2014, 8, 12004. Wang *et al.* *ACS nano*. 2017, 11, 1728), the FEP materials are attached to other plates which will vibrate with the vibration sources. But it's difficult for the plates with heavy masses to vibrate in the very low-amplitude vibration. But in this work, the periphery of the FEP film is fixed and its center effective working area can vibrate freely with the vibration excitation. The VS-TENG vibrates with the vibration source at first, and then the FEP film interacts with the air to vibrate subsequently. That's why the film need to be lightweight and sensitive to air pressures. And the foamed aluminum is used as the other tribo-charge layer, whose porous structure can effectively increase the contact area and reduce the air damping applied on the vibration film. Therefore, even in very low-amplitude vibrations, the FEP film can also vibrate with the vibration sources, and the TENG can work well. The output performance of the TENG with foamed aluminum is much better than that with the normal aluminum. Figure N2 shows the comparison of the electrical signals output by the TENGs (after filtering 50 Hz noises) using different electrodes. For each figure, the blue, orange and green curves are the signals output by the TENG using normal aluminum (Figure N2a), normal aluminum with air holes (Figure N2b), and foamed aluminum (Figure N2c). The output of the TENG using aluminum with air holes is much better than that using normal aluminum, and the TENG using the foamed aluminum has the best output performance (Figure N2d-l). It is worth to note that here the vibration sensor is different from the acoustic sensor. Because the vibration sensor is excited by the acceleration from the vibration source, then the internal structure of the TENG can interact with the air, while the acoustic sensor is directly excited by the sound pressure.

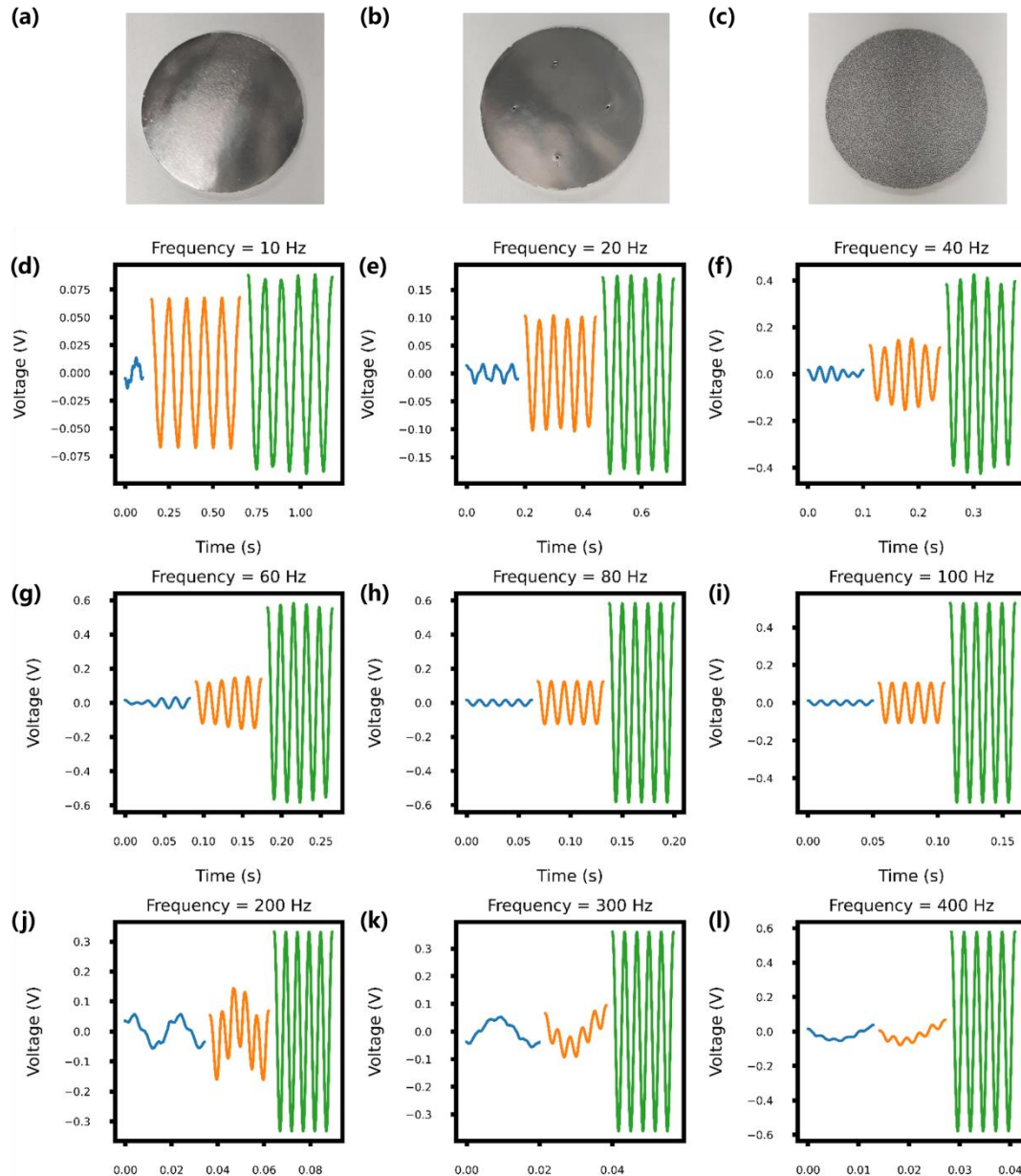


**Figure N2.** The comparison of the electrical signals output by the TENGs using different electrodes. Photograph of a) normal aluminum, b) aluminum with air holes and c) foamed aluminum. The open-circuit voltage of the TENGs using different electrodes at d) 10 Hz, e) 20 Hz, f) 40 Hz, g) 60 Hz, h) 80 Hz, i) 100 Hz, j) 200 Hz, k) 300Hz and l) 400 Hz.

### **Supplementary Note S3. The calculation of the amplitude**

It should be noted here that the minimum vibration amplitude is measured indirectly, which is calculated from the frequency and acceleration. For the relationship between the vibration frequency, acceleration and amplitude is  $B = A\omega^2$ , where  $B$  is the peak value of acceleration,  $A$  is amplitude, and  $\omega = 2\pi f$  is the angular frequency of vibration. In the experiment, the vibration exciter is driven by a signal generator and a power amplifier. The vibration frequency is controlled by the signal generator and the acceleration is detected by an accelerometer provided by the same manufacturer as the vibration exciter. After the frequency and acceleration are confirmed, the amplitude can be calculated from their mathematical relationship. In Figure 3d-f, the main vibration parameters for each point are determined. For Figure 3d-f, when the frequency is 400 Hz and acceleration is 20 m/s<sup>2</sup> (RMS value), the amplitude can be calculated as 4.48 μm, in which case the instantaneous signal is shown in Figure 3d. When the frequency is 1000 Hz and acceleration is 15 m/s<sup>2</sup>, with the instantaneous signal shown in Figure 3e, the amplitude can be calculated as 0.54 μm. And when the frequency is 2000 Hz and acceleration is 10 m/s<sup>2</sup>, the amplitude can be calculated as 89.6 nm. The instantaneous signal is shown in Figure 3f, demonstrating that the VS-TENG can detect low-amplitude vibrations.

#### **Supplementary Note S4. The working mechanism for the VS-TENG in low amplitude vibration condition**

The working principle of the TENG is based on both contact triboelectrification and electrostatic induction. At the first working cycles of the TENG, the dielectric material and the metal electrode must be contacted for contact electrification so that charge transfer occurs between the dielectric material and metal electrode interface. At the same time, charge transfer occurs at the external circuit. After that, the built-in electric field is established inside of the TENG. The inside of the TENG is controlled by displacement current, while the current detected in the external circuit is capacitive conduction current. The internal and external circuits can meet at electrodes to form a complete loop. At every quasi-static moment, the entire TENG system consisting of the built-in electric field and the external circuit reaches an electrostatic equilibrium state. While when the TENG is triggered by the vibration force, the dielectric film moves and the distance between the two materials changes. In this case, the built-in electric field changes and the electrostatic equilibrium state is broken, so there will be charge transfer in the external circuit. The distance between the dielectric film and the metal electrode is 100  $\mu\text{m}$ . But even in the low amplitude vibration, for example, the instantaneous signal in Figure 3d is measured under the vibration amplitude of 4.48  $\mu\text{m}$ , the TENG can also have a stable output with the working mechanism of electrostatic induction.

**Supplementary Note S5. The continuous frequency response of the sensor by sweeping frequency.**

Using the signal generator to sweep frequency and drive the vibration exciter to generate continuously varying vibration is a method to study the frequency response of the TENG. We have added the experiment and the continuous frequency response of the sensor is shown in Figure N3. However, in the frequency sweeping process, after the signal generator automatically changes the frequency, the impedance of the exciter also changes with the vibration frequency. Therefore, for a certain moment in the frequency sweeping process, only the vibration frequency is known, while the acceleration and amplitude are unknown. For Figure 3d-3f, in the experiment, every time the vibration frequency is changed, the acceleration is recalibrated using the accelerometerto control the acceleration. For each discrete point, its vibration frequency and acceleration are known, and the amplitude can be calculated by the formula, so we can intuitively know the vibration condition of each point.

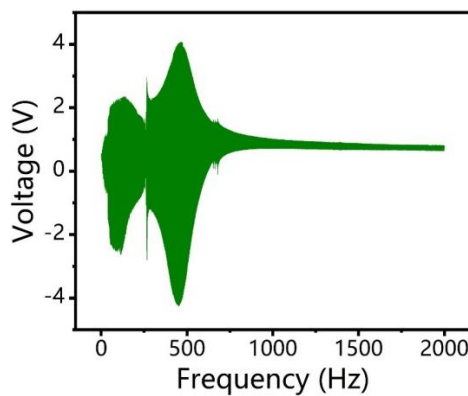


**Figure N3.**The continuous frequency response of the sensor by sweeping frequency.

### **Supplementary Note S6. The output performance of the VS-TENG at different temperatures and humidity.**

Previous study shows that when the temperature increase, the electrical output of the TENG will decrease due to the thermionic electron emission (Wang *et al. Materials Today*. 2019, 30, 34). The voltage of the VS-TENG also decreases with the temperature (Figure N4a-b), but it still has high stability at high temperatures. For the TENGs whose tribo-charge layers are exposed to air, their electrical output will decrease significantly with the increase of the humidity, because the humidity can influence the contact electrification of the tribo-charge layers (Wang *et al. Nano Energy*. 2022, 93, 106880). But the tribo-charge layers of the TENG are not exposed to air, so it can work stably in a high humidity (Figure N4c-d). When the humidity increase, the voltage of the VS-TENG also increases, this may be due to the humidity may influence the activity of the electrons on the gold electrode. The similar experimental result can also be found in the reference “Lai *et al. Nano Energy*. 2019, 60, 715”. In fact, it should be noted here that the main feature we want to detect in this application scenario is the signal frequency, which will not be affected by the humidity and temperature. Generally high-frequency machines are prone to heat, so in the area where machinery and equipment are concentrated, such as ship engine rooms, the ambient temperature is usually 35-50 degrees Celsius. The voltage of the VS-TENG will decrease with the increase of the temperature, but it still has high stability at high temperatures. In the experiment of detecting the vibration of the air compressor, the metal shell of the air compressor also has a high temperature. But the TENG also has a PLA shell, and its tribo-charge layers are not in direct contact with the mechanical device. Therefore, the TENG can work normally to detect the vibration of the air compressor. With the stable electrical output in high temperatures, we can also eliminate the effect of temperature on the electrical output of the TENG through algorithms, or we can encapsulate the TENG with thermal insulation materials to solve the problem caused by the high temperature.

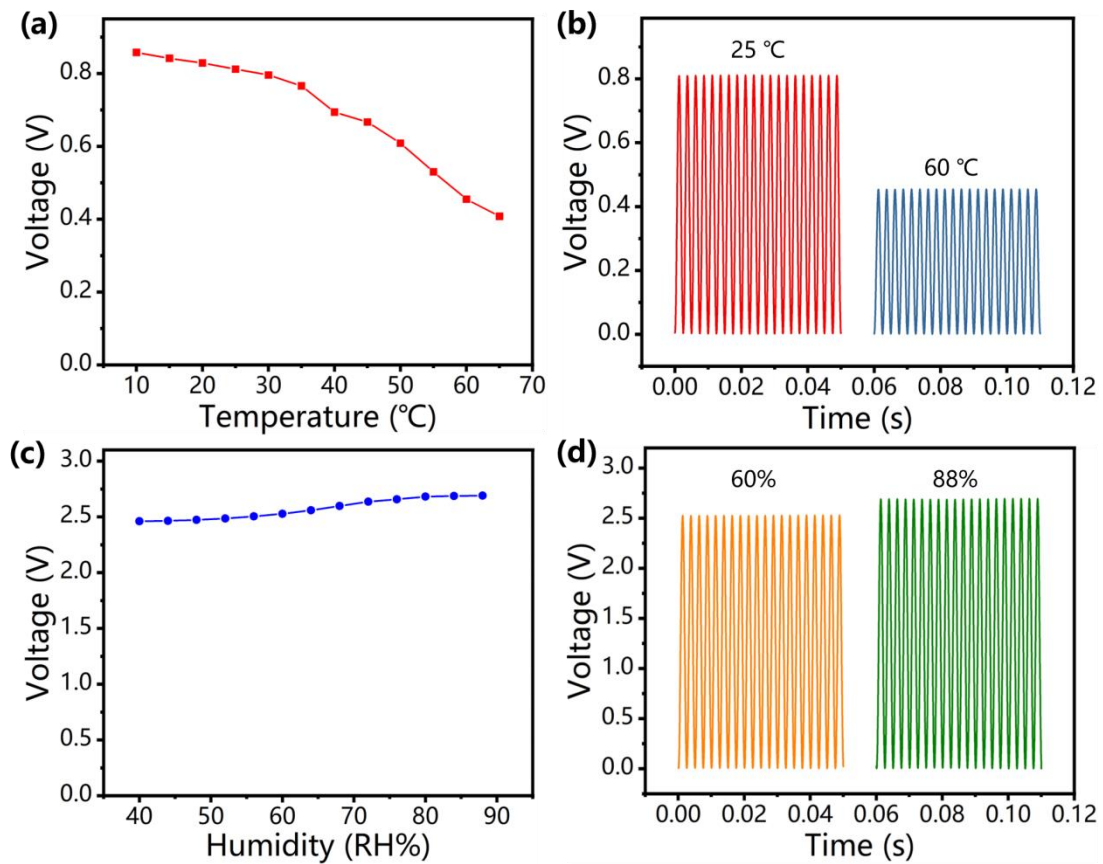


**Figure N4.**The electrical output of the TENG at different temperatures and humidity. a) Variation of the open-circuit voltage with temperature. b) Instantaneous signals of the TENG at different temperatures. c) Variation of the open-circuit voltage with humidity. d) Instantaneous signals of the TENG at different humidity.

**Supplementary Note S7. Calculation progress of the voltage frequency.**

For the real-time monitoring experiment, the frequency of the output voltage is indeed detected simultaneously. To better illustrate the mechanism, the detailed detection and estimation process is explained as follows. The voltage of the TENG is measured by the electrometer, and the data is sent to the computer and displayed in the LABVIEW software. Since the LABVIEW has an interface with the MATLAB software, the Fourier transform of the data is performed by MATLAB, which returns the calculation results (the frequencies of the voltage signals) every 0.1 s. With a sampling rate of 20,000 Hz, 2,000 data are processed simultaneously, in MATLAB software the processing time can be ignored. After the frequency of the voltage is obtained, the vibration acceleration can be calculated according to the frequency and the voltage value (recognized by MATLAB). Furthermore, the vibration amplitude can also be calculated from the vibration frequency and acceleration.

### Supplementary Note S8. The energy conversion algorithm of the TENG system.

The proposed algorithm does not rely on the linearity of the sensor response, with which the vibration parameters and the voltage of the TENG can be mutually calculated from each other. In other words, if we regard the TENG as a system, the parameters inputting the system are the basic parameters of mechanical motion (frequency, acceleration, amplitude for the VS-TENG), and the parameters outputting the system are voltage, current and transferred charge. For the VS-TENG, when the motion of the vibration source is sinusoidal, the electrical output of the VS-TENG is also a sinusoidal signal with the same frequency. But at different frequencies, the conversion efficiency is not the same (due to the sensitivity varies with the frequency), so the relationship between the voltage and vibration parameters is:

$$V = \alpha A(f, a), \quad (\text{N1})$$

where  $V$  is the voltage of the VS-TENG,  $A$  is the equivalent system conversion function of the TENG (for mechanical vibration signals converting to electrical signals),  $\alpha$  is the conversion factor fitted from the voltage sensitivity in different frequencies (Figure R1a),  $f$  is the frequency and  $a$  is acceleration. For the sinusoidal signals, we can read the voltage  $V$  and the frequency  $f$  is obtained by the Fourier transform (Supplementary Movie 1), thus we can get the vibration acceleration and furtherly the vibration amplitude can be calculated.

However, for the complex signals, we need further analysis. We know that any signal can be represented by a set of sinusoidal signals of different frequencies, so we can do the Fourier transform on the vibration signal (Figure N5i) to obtain the intensity values of different frequency components (Figure N5ii):

$$\hat{a}(f) = \int a(t) e^{-j2\pi f t} dt, \quad (\text{N2})$$

$$\hat{a}(k) = \sum a(n) e^{j\frac{2\pi}{N} nk}, \quad (\text{N3})$$

With each vibration component entering the system, it outputs an electrical component with the same frequency and different amplitude (Figure N5iii):

$$\hat{V}(f_i) = \alpha \hat{a}(f_i) A(f_i), \quad (\text{N4})$$

With these electrical components, we can get the entire output signal of TENG through the inverse Fourier transform (Figure N5iv):

$$V(t) = \frac{1}{2\pi} \int \hat{V}(f) e^{j2\pi f t} df, \quad (\text{N5})$$

$$V(n) = \frac{1}{N} \sum \hat{V}(k) e^{j\frac{2\pi}{N} nk}, \quad (\text{N6})$$

Eq. (N2) and Eq. (N5) are used for the calculation of continuous signals, and Eq. (N3) and Eq. (N6) are used for the calculation of discrete signals. Since the algorithm is based on the

Fourier transform and inverse Fourier transform, the signals can be processed quickly by the computer.

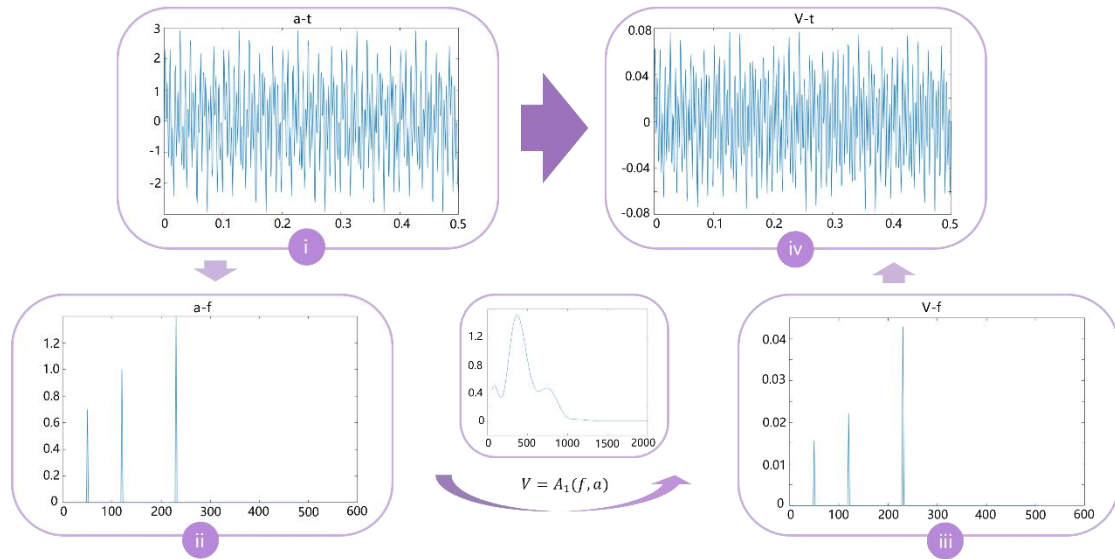


**Figure N5.** Calculation process for the energy conversion algorithm of the TENG system.

**Supplementary Note S9. Comparison of the original signal and the voltage signal after working 1000000 cycles.**

In the experiment, the vibration frequency is 500 Hz and the totally time is 2000 s. In order not to cause data storage problems of the computer, the data is saved every 500 seconds. The voltage signals of the TENG for working 2000 s are shown in Figure N7a. After the TENG working for 2000 s, we use the accelerometer to recalibrate the vibration of the exciter ( $20 \text{ m/s}^2$ ) to ensure it is the same as the previous vibration. The comparison of the original signal and the signal after working 2000 s is shown in Figure N7b.

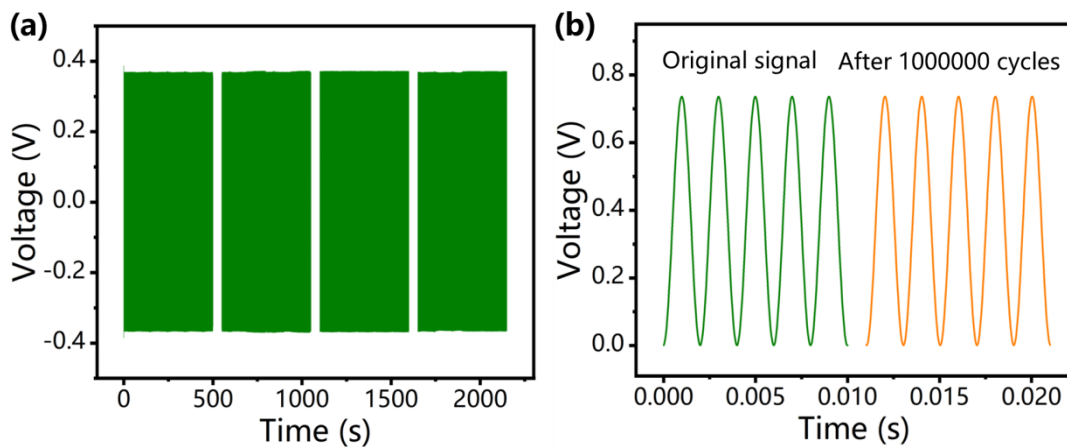


**Figure N6.** a) The voltage signals of the TENG for working 2000 s. b) The comparison of the original signal and the signal after working 2000 s.